



Locating the critical end point of QCD

Christian S. Fischer^a, Jan Luecker^{b,c}, Christian A. Welzbacher^a

^a*Institut für Theoretische Physik, Justus-Liebig-Universität Gießen, Heinrich-Buff-Ring 16, D-35392 Gießen, Germany.*

^b*Institut für Theoretische Physik, Universität Heidelberg, Philosophenweg 16, D-69120 Heidelberg, Germany.*

^c*Institut für Theoretische Physik, Goethe-Universität Frankfurt, Max-von-Laue-Straße 1, D-60438 Frankfurt/Main, Germany*

Abstract

We summarize recent results for the phase structure of QCD at finite temperature and light-quark chemical potential for $N_f = 2 + 1$ and $N_f = 2 + 1 + 1$ dynamical quark flavors. We discuss order parameters for the chiral and deconfinement transitions obtained from solutions of a coupled set of (truncated) Dyson-Schwinger equations for the quark and gluon propagators of Landau gauge QCD. Based on excellent agreement with results from lattice-QCD at zero chemical potential we study the possible appearance of a critical end-point at large chemical potential.

Keywords: Critical end point, QCD phase diagram, Dyson-Schwinger equations

1. Introduction

Heavy ion collision experiments at BNL, LHC and the future FAIR facility are designed to probe the properties of the quark-gluon plasma (QGP) and the transition from (almost) chirally symmetric and deconfined matter into the chirally broken and confined states of the hadronic phase. At the very large energies available at the LHC, in principle two entire quark families have to be taken into account in the theoretical description of these experiments via the equation of state. However, even at smaller temperatures at or above the light-quark crossover region, the effects of charm quarks on the EoS and the transition temperatures may not be entirely negligible. First lattice studies for $N_f = 2 + 1 + 1$ flavors indicate indeed, that charm quarks may not be treated in the quenched approximation, i.e. the back-reaction of the charm quarks onto the Yang-Mills sector of the theory is quantitatively important [1].

In this contribution we summarize recent results on the QCD phase diagram via a framework of Dyson-Schwinger equations (DSEs) for the quark and gluon propagator of Landau gauge QCD. We discuss the phase diagram for $N_f = 2 + 1$ flavors and estimate the influence of the charm quark on the phase structure of QCD and the location of a putative critical end-point. While the approach is first principle, truncations have to be introduced to convert the equations into a form suitable for practical calculations. In order to make these approximations well controlled we use constraints such as symmetries and conservation laws as well as comparison with corresponding results from lattice calculations (where available). Our aim is to tighten this control to such extent that reliable results for large chemical potential become feasible. One of the advantages of our framework over model treatments (see e.g. Ref [2] and Refs. therein) is the direct accessibility of the Yang-Mills sector of QCD thus rendering a fully dynamical treatment of all members of the first two quark families feasible. For corresponding efforts in the functional renormalization group approach see e.g. [3, 4, 5, 6, 7, 8] and the overview of Jan Pawłowski in these proceedings [9].

This contribution is organized as follows. In the next section we summarize our approach, details can be found in [10, 11, 12, 13, 14]. In section 3 we discuss results for $N_f = 2 + 1$ quark flavors and compare with lattice QCD. We also study the effects of the charm quarks onto the QCD phase diagram.

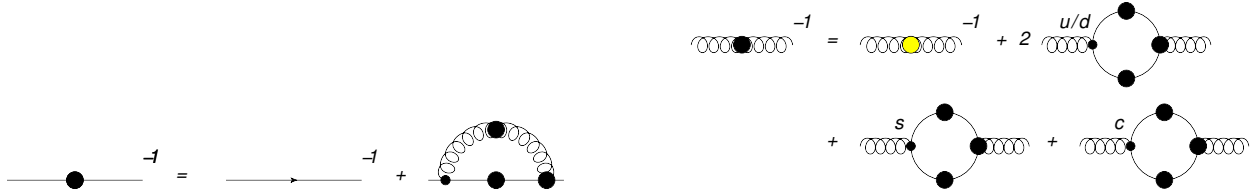


Figure 1. Left: The DSE for the quark propagator. Large blobs denote dressed propagators and vertices. Right: The truncated gluon DSE for $N_f = 2 + 1 + 1$ QCD. The light shaded (yellow) dot denotes the quenched (lattice) propagator.

2. Framework

The DSEs for the quark and gluon propagators are displayed in Fig. 1. The fully dressed propagators on the left hand side of the equations are determined from the diagrams on the right hand side, which include the corresponding bare propagators as well as loops representing integrals in momentum space over non-perturbative propagators and vertices. In the quark-DSE the essential ingredients are the fully dressed gluon propagator as well as the dressed quark-gluon vertex. The appearance of the dressed quark propagator also inside the loop renders the equation self-referential. We solve one quark-DSE iteratively for each of the N_f quark flavors involved in the calculation.

At the same time, each quark flavor is back-coupled onto the gluon propagator according to the gluon-DSE displayed in the right part of Fig. 1 for the case of $N_f = 2 + 1 + 1$. The key idea of our truncation of the gluon DSE is to replace the self-energy loops containing only Yang-Mills propagators and vertices with the quenched gluon propagator obtained from lattice calculations. This procedure simplifies the numerical task dramatically and guarantees that the important physics of temperature effects in pure Yang-Mills theory is contained in our approximation scheme. In addition, we use an ansatz for the quark-gluon vertex which contains temperature and chemical potential effects according to (approximated) Slavnov-Taylor identities; see Ref. [12] for details. This construction for the vertex contains one open parameter, which controls the interaction strength of the vertex at low momentum. This parameter can be fixed in two ways: either it is chosen such that the pseudo-critical temperature of the chiral transition extracted from $N_f = 2 + 1$ -lattice calculations is reproduced, or it can be fixed from experimental input for the pion decay constant at zero temperature. The difference between these two methods is a signal for the systematic error of our calculation and is at the level of ten to fifteen percent for the pseudo-critical temperatures at zero chemical potential.

3. Results

The quality of our approach may be assessed from the results for the unquenched gluon propagator at finite temperature calculated in Ref. [12]. In Fig. 2 we show the part of the propagator longitudinal to the heat bath evaluated for $N_f = 2$ and a heavy pion mass of $m_\pi = 316$ MeV compared to corresponding lattice calculations of Ref. [15]. As can be seen from the plot and is discussed in detail in Ref. [14], both calculations match very well. We wish to emphasize that the DSE results appeared before the lattice data and therefore constituted a prediction for the unquenched gluon.

Next we discuss the results for the chiral and deconfinement transition with $N_f = 2 + 1$ physical up/down and strange quark masses [14]. In the right diagram of Fig. 2 we display the regularized quark condensate as well as the Polyakov loop as a function of temperature at zero chemical potential. We find excellent agreement with the lattice data. Here the strength of the quark-gluon interaction has been adjusted such that the (pseudo)-critical transition temperature of the lattice data is reproduced. A non-trivial result, however, is the agreement of the slope of the chiral transition of the DSE results with the lattice data (see Ref. [8] for a corresponding agreement within the PQM model). Together with the results for the unquenched gluon this demonstrates that our truncation scheme works well at zero chemical potential. The resulting transition temperatures extracted from the chiral susceptibility and the inflection point of the light quark condensate are given by

$$T_c \Big|_{\frac{d\langle\bar{\psi}\psi\rangle}{dT}} = 160.2 \text{ MeV}, \quad T_c \Big|_{\frac{d\langle\bar{\psi}\psi\rangle}{dT}} = 155.6 \text{ MeV}. \quad (1)$$

Our results for the QCD phase diagram at finite chemical quark potential are shown in the left diagram of Fig. 3 using the inflection point of the light quark condensate to pin down the transition temperature for the chiral transition

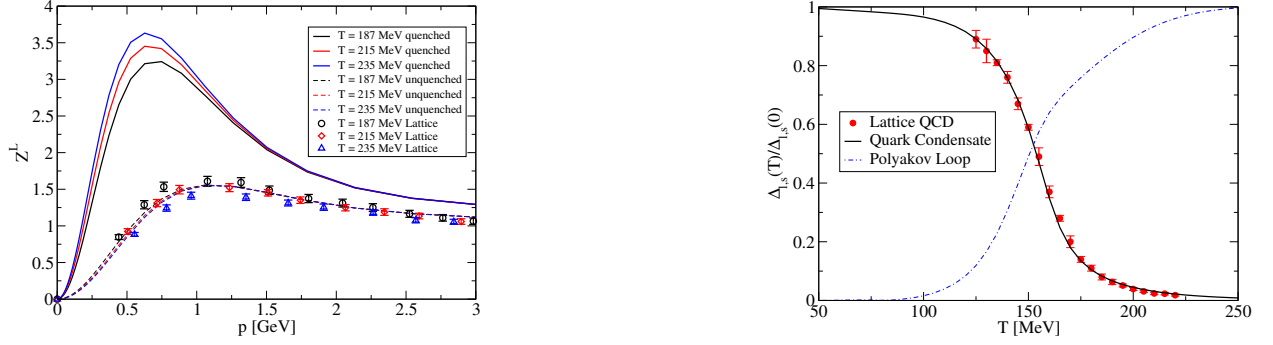


Figure 2. Left diagram: comparison of electric gluon dressing function for $N_f=2$ in the DSE approach [13] with lattice data [15]. All results have been evaluated at a pion mass of $m_\pi = 316$ MeV. Right diagram: regularized chiral condensate and the Polyakov loop for $N_f = 2 + 1$ quark flavors as a function of temperature at zero quark chemical potential $\mu_q = 0$. The interaction strength of the quark-gluon vertex is fixed to reproduce the critical temperature of the lattice results of Ref. [16]. Both figures are adapted from Ref. [14].

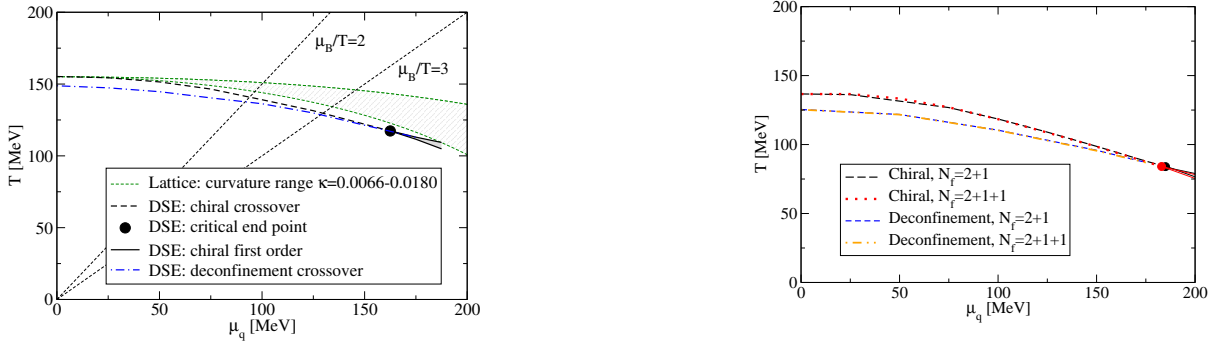


Figure 3. Left diagram: phase diagram for $N_f = 2 + 1$ quark flavors. Shown are our results together with an extrapolation of a range of curvatures for the chiral transition extracted at imaginary and small chemical potential from different lattice groups [17, 18, 19]. Right diagram: comparison between $N_f = 2 + 1$ and $N_f = 2 + 1 + 1$ flavors, where in both cases the interaction strength of the quark-gluon vertex and the quark masses are fixed to reproduce vacuum physics. Both figures are adapted from Ref. [14].

and the Polyakov loop potential for the corresponding one for deconfinement. The chiral crossover, displayed by the dashed black line turns into a chiral critical end point (CEP) at

$$(T^c, \mu_q^c) = (115, 168) \text{ MeV}, \quad (2)$$

where also the deconfinement transition line meets the chiral one. To better guide the eye, we have also plotted lines with ratios of baryon chemical potential over temperature $\mu_B/T = 2$ and $\mu_B/T = 3$.

In order to assess the quantitative reliability of our result for the CEP some comments are in order. In the current approximation for the quark-gluon vertex we relied on a construction that is built along its Slavnov-Taylor identity, but does not yet encode explicitly the effects of the back-coupling of mesons and baryons onto the quark propagator (see e.g. Refs. [20, 21, 22] for first studies of these effects). At $\mu = 0$ and finite quark mass it appears not to be necessary to include these effects explicitly, as demonstrated by the agreement with the quark condensate from the lattice. However, finite chemical potential, meson and baryon effects in the quark-gluon vertex may introduce additional dependence on chemical potential on top of the one already covered by our ansatz. It certainly needs to be studied in future work, whether these contributions have a large impact onto the location of the critical end point.

In Fig. 3 we also compare our result for the chiral transition line with lattice results of its curvature determined around $\mu = 0$ and extrapolated to finite chemical potential [17, 18, 19]. Although the overall agreement of the lattice extrapolation with our results is quite satisfactory one should bear in mind the above caveats. Similar caveats may apply to the lattice extrapolations, since the effects of baryons onto the curvature may only set in at large chemical potential and may therefore not be captured by the extrapolation.

The effects of charm quarks onto the chiral transition line can be assessed from the diagram on the right hand side of Fig. 3. To this end we fixed both, the interaction strength of the quark-gluon vertex for $N_f = 2 + 1$ and $N_f = 2 + 1 + 1$ to the physical pion decay constant. As mentioned above, this leads to a decrease of the chiral transition temperature by about $\Delta T \approx 20$ MeV compared to the results discussed above. On the other hand, this procedure taking care of the change of scale when going from $N_f = 2 + 1$ to $N_f = 2 + 1 + 1$ allows us to directly compare the phase diagram with and without charm quarks. As a result we find that the influence of the charm quark on the chiral and deconfinement transition is almost negligible apart from a very small shift of the critical end point towards smaller chemical potential still within the limits of numerical uncertainty¹. We expect to see a similar behavior in corresponding future lattice calculations.

Acknowledgments

This work has been supported by the Helmholtz International Center for FAIR within the LOEWE program of the State of Hesse.

References

- [1] C. Ratti, S. Borsanyi, G. Endrodi, Z. Fodor, S. D. Katz, et al., Lattice QCD thermodynamics in the presence of the charm quark, Nucl.Phys. A904-905 (2013) 869c–872c. doi:10.1016/j.nuclphysa.2013.02.153.
- [2] S.-x. Qin, L. Chang, H. Chen, Y.-x. Liu, C. D. Roberts, Phase diagram and critical endpoint for strongly-interacting quarks, Phys.Rev.Lett. 106 (2011) 172301. arXiv:1011.2876, doi:10.1103/PhysRevLett.106.172301.
- [3] J. Braun, L. M. Haas, F. Marhauser, J. M. Pawłowski, Phase structure of two-flavor QCD at finite chemical potential, Phys.Rev.Lett. 106 (2011) 022002. arXiv:0908.0008, doi:10.1103/PhysRevLett.106.022002.
- [4] J. Braun, H. Gies, J. M. Pawłowski, Quark Confinement from Color Confinement, Phys.Lett. B684 (2010) 262–267. arXiv:0708.2413, doi:10.1016/j.physletb.2010.01.009.
- [5] T. K. Herbst, J. M. Pawłowski, B.-J. Schaefer, The phase structure of the Polyakov–quark–meson model beyond mean field, Phys.Lett. B696 (2011) 58–67. arXiv:1008.0081, doi:10.1016/j.physletb.2010.12.003.
- [6] T. K. Herbst, J. M. Pawłowski, B.-J. Schaefer, Phase structure and thermodynamics of QCD, Phys.Rev. D88 (1) (2013) 014007. arXiv:1302.1426, doi:10.1103/PhysRevD.88.014007.
- [7] L. Fister, J. M. Pawłowski, Confinement from Correlation Functions, Phys.Rev. D88 (2013) 045010. arXiv:1301.4163, doi:10.1103/PhysRevD.88.045010.
- [8] T. K. Herbst, M. Mitter, J. M. Pawłowski, B.-J. Schaefer, R. Stiele, Thermodynamics of QCD at vanishing density, Phys.Lett. B731 (2014) 248–256. arXiv:1308.3621, doi:10.1016/j.physletb.2014.02.045.
- [9] J. M. Pawłowski, work in progress.
- [10] C. S. Fischer, Deconfinement phase transition and the quark condensate, Phys.Rev.Lett. 103 (2009) 052003. arXiv:0904.2700, doi:10.1103/PhysRevLett.103.052003.
- [11] C. S. Fischer, A. Maas, J. A. Müller, Chiral and deconfinement transition from correlation functions: SU(2) vs. SU(3), Eur.Phys.J. C68 (2010) 165–181. arXiv:1003.1960, doi:10.1140/epjc/s10052-010-1343-1.
- [12] C. S. Fischer, J. Luecker, Propagators and phase structure of Nf=2 and Nf=2+1 QCD, Phys.Lett. B718 (2013) 1036–1043. arXiv:1206.5191, doi:10.1016/j.physletb.2012.11.054.
- [13] C. S. Fischer, L. Fister, J. Luecker, J. M. Pawłowski, Polyakov loop potential at finite density, Phys.Lett. B732 (2014) 273–277. arXiv:1306.6022, doi:10.1016/j.physletb.2014.03.057.
- [14] C. S. Fischer, J. Luecker and C. A. Welzbacher, Phase structure of three and four flavor QCD, Phys. Rev. D90 (2014) 034022, arXiv:1405.4762 [hep-ph], doi:10.1103/PhysRevD.90.034022.
- [15] R. Aouane, F. Burger, E.-M. Ilgenfritz, M. Müller-Preussker, A. Sternbeck, Landau gauge gluon and ghost propagators from lattice QCD with Nf=2 twisted mass fermions at finite temperature, Phys.Rev. D87 (2013) 114502. arXiv:1212.1102, doi:10.1103/PhysRevD.87.114502.
- [16] S. Borsanyi, et al., Is there still any T_c mystery in lattice QCD? Results with physical masses in the continuum limit III, JHEP 1009 (2010) 073. arXiv:1005.3508, doi:10.1007/JHEP09(2010)073.
- [17] G. Endrodi, Z. Fodor, S. Katz, K. Szabo, The QCD phase diagram at nonzero quark density, JHEP 1104 (2011) 001. arXiv:1102.1356, doi:10.1007/JHEP04(2011)001.
- [18] O. Kaczmarek, F. Karsch, E. Laermann, C. Miao, S. Mukherjee, et al., Phase boundary for the chiral transition in (2+1)-flavor QCD at small values of the chemical potential, Phys.Rev. D83 (2011) 014504. arXiv:1011.3130, doi:10.1103/PhysRevD.83.014504.
- [19] P. Cea, L. Cosmai, A. Papa, On the critical line of 2+1 flavor QCD, Phys.Rev. D89 (2014) 074512. arXiv:1403.0821, doi:10.1103/PhysRevD.89.074512.
- [20] C. S. Fischer, D. Nickel, J. Wambach, Hadronic unquenching effects in the quark propagator, Phys.Rev. D76 (2007) 094009. arXiv:0705.4407, doi:10.1103/PhysRevD.76.094009.
- [21] C. S. Fischer, R. Williams, Beyond the rainbow: Effects from pion back-coupling, Phys.Rev. D78 (2008) 074006. arXiv:0808.3372, doi:10.1103/PhysRevD.78.074006.

¹If instead we kept the interaction strength and scale of the $N_f = 2 + 1$ case and merely added the charm quark we would have obtained a shift of the transition line towards smaller temperatures of about $\Delta T \approx 23$ MeV.

- [22] C. S. Fischer, J. A. Mueller, On critical scaling at the QCD $N_f = 2$ chiral phase transition, *Phys.Rev. D*84 (2011) 054013. [arXiv:1106.2700](#), [doi:10.1103/PhysRevD.84.054013](#).